ISSN 1063-7729, Astronomy Reports, 2011, Vol. 55, No. 11, pp. 978–988. © Pleiades Publishing, Ltd., 2011.
Original Russian Text © I.D. Litovchenko, A.V. Alakoz, I.E. Val'tts, G.M. Larionov, 2011, published in Astronomicheskii Zhurnal, 2011, Vol. 88, No. 11, pp. 1061–1072.

Search for Class I Methanol Maser Emission toward Several Supernova Remnants

I. D. Litovchenko*, A. V. Alakoz, I. E. Val'tts, and G. M. Larionov

Astro Space Center, Lebedev Physical Institute, Russian Academy of Sciences, Profsoyuznaya ul. 84/32, Moscow, 117997 Russia

Received March 18, 2011; in final form, April 11, 2011

Abstract—Observations at 44 GHz in the $7_0-6_1A^+$ methanol line have been carried out on the 20-m telescope of the Onsala Space Observatory (Sweden) in the directions of the poorly studied region G27.4-0.2 and of several supernova remnants, at the coordinates of the OH(1720) maser satellite emission, with the aim of searching for Class I methanol maser emission in these sources. The region G27.4-0.2 has been mapped, and contains maser sources and two supernova remnants with similar coordinates and radial velocities, which may accelerate condensation of the ambient gas–dust medium. This may play a role in enhancing the probability of methanol formation and maser emission. This is the first detection of 44 GHz maser emission in this source, and this maser is among the 10% of the strongest Class I methanol masers, within the uncertainties in the integrated flux (of a total of 198 currently known masers). A $27' \times 27'$ region around the maser has been mapped at 44 GHz in steps of $1'$. The 44-GHz emission forms only within the previously known maser region. Further studies in water lines are needed to estimate the influence of shocks from supernovae. No 44-GHz Class I methanol maser emission was detected at the 3σ level at the coordinates of the OH(1720) satellite emission in six supernova remnants; i.e., the presence of OH(1720) emission is not a sufficient condition for the detection of Class I methanol masers.

DOI: 10.1134/S1063772911110059

1. INTRODUCTION

Turbulent phenomena in the form of bipolar outflows, curved arcs or half-rings of matter, or other complex vortical motions in which the interaction between shocks and the surrounding matter can be traced are often observed in the vicinity of young stellar objects. These formations represent energetically powerful processes, which should influence gas–dust clumps embedded in these molecular clouds and the chemical–physical processes occurring in them. A shock front leads to the motion of numerous dense filaments, scattering and accelerating them on a range of scales and speeds. Heated condensations will radiatively cool in lines of CO and SiO, which can act as tracers of the motions in the medium, as well as in lines of CS and NH_3, which trace the presence of dense gas. Broad spectra of rotational and oscillational lines of H_2 are observed at shock fronts. Molecular hydrogen traces gas perturbed by collisions of various flows with the molecular clouds. In particular, shocks can excite emission in the $v = 1-0$ $S(1)$ line of H_2 at 2.12 μm. Emission in this line indicates the presence of a shock front associated with a bipolar outflow or other active, dynamical process in the medium surrounding a condensation. Note that, although H_2 can be excited by the passage of moving material through a medium, it can also be excited by UV radiation from nearby ultra-compact HII regions [1]. However, the zone of H_2 emission has a different appearance in this case: shock-induced H_2 emission should be observed far from stars, while UV-induced H_2 emission should be observed in the immediate vicinity of the exciting stars. Special spectral techniques based on the analysis of hydrogen-line profiles and intensity ratios can be used to distinguish between emission associated with flourescence and with shocks [2].

According to our current understanding, complex organic molecules, in particular methanol, can be formed in dense condensations in molecular clouds, in places where high-velocity shock fronts and flows are decelerated. Methanol can be observed at many frequencies and in many transitions, with some of these levels being inverted, giving rise to maser emission. Class I methanol masers (MMIs) are predominantly collisionally pumped [3] (characteristic line frequencies of 25, 36, 44, 84, and 95 GHz), while Class II methonol masers (MMIIs) are predominantly pumped by external radiation from nearby ultra-compact HII regions [4] (characteristic line frequencies of 6.7 and 12.2 GHz).

*E-mail: grosh@asc.rssi.ru

The compression of maser condensations by bipolar outflows can appreciably influence the intensities of MMIs [5, 6], whose pumping is sensitive to variations in the density of the medium. However, shock fronts formed by supernova explosions can also be adopted as targets in searches for MMI emission. In this case, the collisional pumping is provided by the passage of the shock through an adjacent cloud in the vicinity of the supernova remnant.

Targeted searches for MMI emission toward supernova remnants (SNRs) had not been carried out previously, although some associations between SNRs and MMIs are known, for example, in the star-forming regions W43, W44, and W51. The question of associations of MMIIs with SNRs is discussed in [7, 8].

In the catalog of MMIs [9, 10], 31 of 198 sources (16%) are located within 10′ of SNRs, which is about a factor of three smaller than the typical size of an SNR (30′ [11]). However, the relationship between masers and SNRs is not obvious in most of the detected associations, and requires special study. Since MMIs can form groups of sources located within regions up to several arcminutes in size [12], the best approach seems to search in the vicinities of known masers associated with SNRs.

The first goal of our current study was 44-GHz mapping of the MMI emission of G27.369-0.164, which is associated with two SNRs: the candidate SNR G27.3-0.2 (within 5′) and the well known and firmly established SNR G27.4+0.0 (Kes73, within 10′). This maser was detected in the survey of [13] at 95 GHz with a peak flux density of 35 Jy, and had not been studied at 44 GHz. The basis for searching for a relationship between the maser region and these SNRs is the proximity of their coordinates and the fact that the neutral-hydrogen line observed toward the SNRs and the 95-GHz methanol line occupy the same radial-velocity interval; a similar criterion was used, for example, in [14] to establish a connection between OH(1720) maser emission and an SNR. The coordinates and velocities of Kes 73 can be found in [15]. The coordinates of G27.3-0.2 are given in [16], and the rate of recombination lines in one of the numerous HII regions in this region at 5 GHz at those same coordinates is given in [17].

An obvious sign of interactions between SNRs and molecular clouds is OH maser emission at 1720 MHz, which is collisionally pumped (see, for example, [18, 19] and references therein).

There have been a number of successful attempts to search for OH(1720) maser emission toward SNRs, for example, in the plane of the Galaxy in the northern [20] and southern [21] hemispheres and in the Magellanic clouds [22]. Interferometric observations aimed at studying connections between SNRs and molecular clouds have also been carried out (see, for example [23] and references therein). These studies have been motivated to an appreciable degree by successful studies of the fine spatial structure of OH(1720) maser emission with the Very Large Array [24], which revealed 26 unresolved maser spots in the direction of the SNR W28.

At the same time, in the 2009 study of [23], OH(1720) maser emission was detected in only 24 SNRs studied at 1720 MHz using single dishes and interferometers with sensitivities of 5–25 mJy and 35–160 mJy, respectively, which corresponds to no more than 15% of the total number of SNRs.

Searches for MMI emission toward several SNRs in which OH maser emission at 1720 MHz had been observed earlier is the second goal of the current study. The criteria used to select the targets, discussion of our results, and comments about individual sources are presented below.

2. OBSERVATIONS

The observations were carried out on the 20-m radio telescope of the Onsala Space Observatory (Sweden) on December 2–15, 2009 in the $7_0 - 6_1 A^+$ methanol line at a rest frequency of 44 069.4900 MHz, at the maser coordinates

$$\mathrm{RA(J2000)} = 18^{\mathrm{h}}41^{\mathrm{m}}50\overset{\mathrm{s}}{.}90,$$

$$\mathrm{Dec(J2000)} = -05^{\circ}01'28\overset{''}{.}3.$$

The beam width for this telescope at 44 GHz is 88″. The aperture efficiency is 53%, which corresponds to roughly 18 Jy per 1 K of corrected antenna temperature. The spectrometer used was a 1600-channel autocorrelator with a transmission bandwidth of 20 MHz and a frequency resolution of 25 kHz, or 0.18 km/s at 44 GHz. The calibration was carried out using a standard chopper-wheel method, also calculating and applying second-order corrections [25]. The system noise temperature was 50 K, and the system noise temperature during the observations varied from 175 K upward, depending on the hour angle and weather conditions. The observations were conducted in an ON–ON regime with positional modulation. A region 27′ × 27′ in size centered on the maser coordinates was mapped in steps of 1′. To obtain a signal-to-noise ratio of 10 Jy (about 0.5 K), each point was observed for roughly 3.5 min. The coordinates of the OH(1720)-emitting SNRs are presented in Table 4.

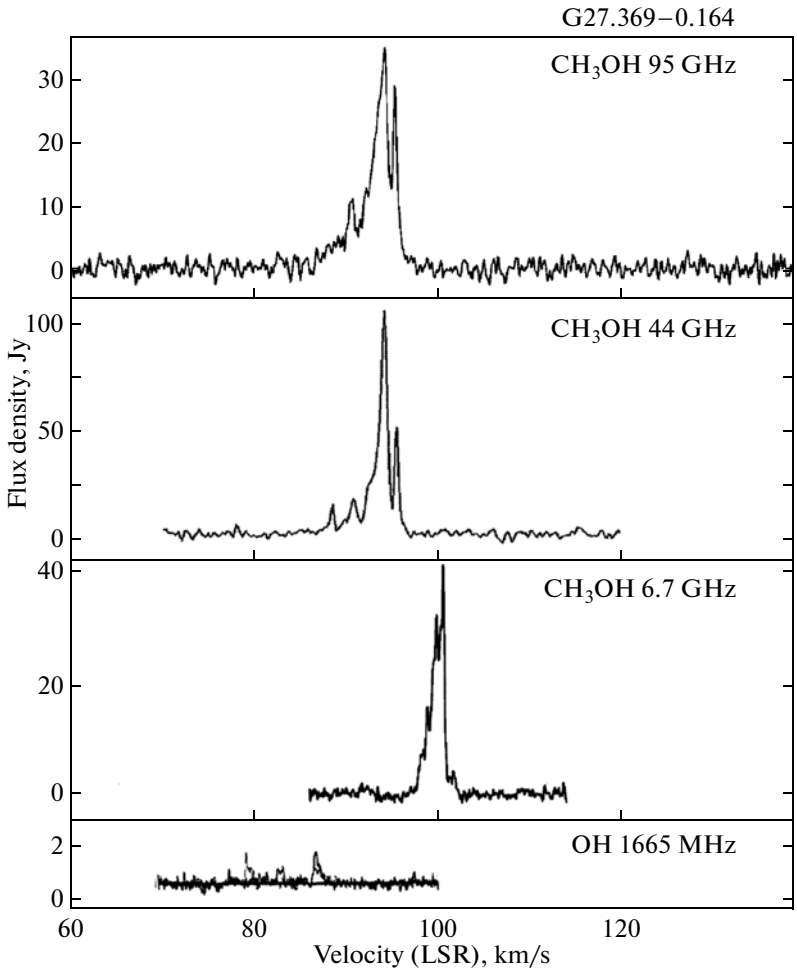

Fig. 1. Methanol-maser spectrum for G37.369−0.164 in the vicinity of the possible SNR G27.3−0.2 and the well known SNR G27.4+0.0 (Kes73) at 6.7 and 95 GHz (taken from [13]). The OH maser spectrum is taken from [26]. The spectrum at 44 GHz was obtained in the current study.

3. MAPPING OF THE G27.4−0.2 REGION: RESULTS

Maser emission was first observed in this star-forming region in the survey of Caswell and Haynes [26], carried out on the 64-m Parkes radio telescope with a 12′ at the frequencies of four hydroxyl lines. Weak OH emission was detected only at 1665 MHz at +98 km/s, near the edge of a diffuse HII region. Ellingsen [13] detected MMII emission at 6.7 GHz with a 7′ beam in this same region, within the pointing uncertainties, as well as MMI emission at 95 GHz on the 22-m Mopra radio telescope, with a beam for the inner 15-m of 52″ [13]. The velocity range for the MMI line was 88–96 km/s, and for the MMII line 88–104 km/s. H_2O maser emission is observed at the same coordinates [27, 28]. The sources IRAS18391-0504 and MSX5C are identified with these masers.

A compact radio source was found in this region in a Galactic-plane continuum survey at 20 cm carried out in 1983 on the VLA in its B configuration [29], which was also detected in a later 5-GHz VLA survey [30].

The maser region is not associated with bipolar outflows—neither in earlier studies (a list of references to methanol masers associated with bipolar outflows is given in the MMI catalog [10]), nor among new candidate bipolar outflows from massive young stellar objects [31]. There are likewise no data indicating bipolar outflows in the direction of this maser in the recent survey [32], which was dedicated to CO (2-1) studies of 98 methanol-maser sources (including this one). We were not able to find observations of this region in thermal lines tracing dense gas (CS, NH_3, or CH_3CN).

We have found MMI emission at 44 GHz at the coordinates of the 95-GHz methanol-maser emission in the Onsala 20-m observations presented here; the spectrum is shown in Fig. 1. For comparison, we also show the methanol spectra at 6.7 GHz and 95 GHz

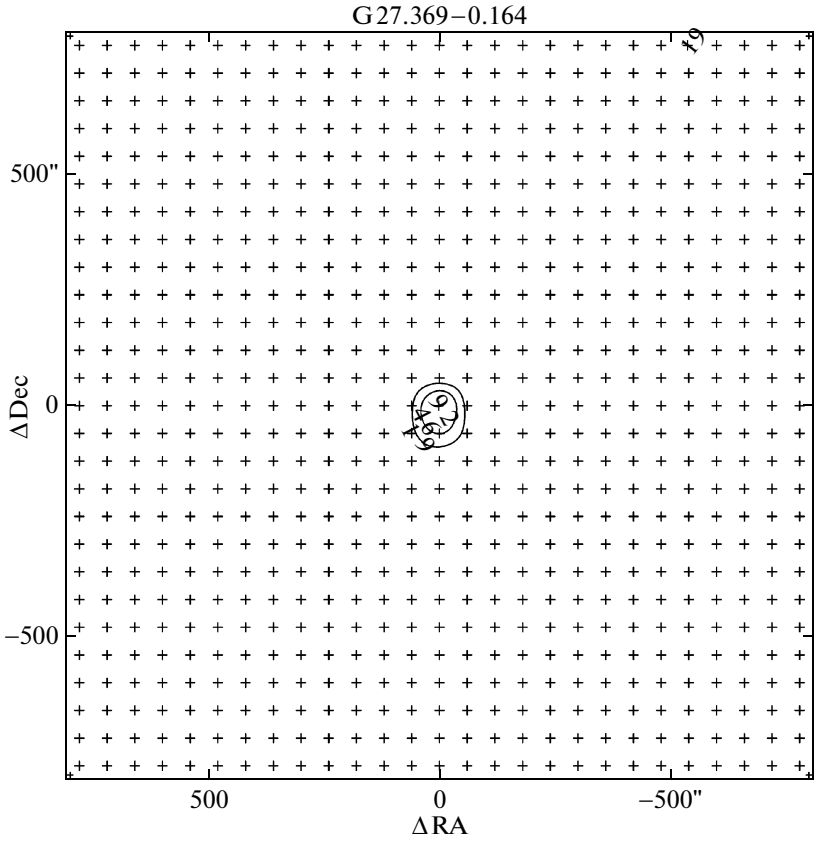

Fig. 2. Map of the vicinity of the MMI emission of G27.369−0.164 in the $7_0 - 6_1A^+$ at 44 GHz. The axes plot distances from the map center (RA(J2000) = $18^h41^m50.90^s$, Dec(J2000) = $-05°01'28.''3$) in arcseconds. A total of 729 positions were observed to produce the $27' \times 27'$ map. The pointing positions were separated by $1'$, and are marked by dots. Three contours corresponding to 20, 50, and 100% of the integrated observed intensity are shown.

from [13] and the OH spectrum from [26]. The maser features at 44 GHz are concentrated at velocities from 88 to 96 km/s. The flux at the peak of the brightest line, at 94.5 km/s, is 130 Jy, which exceeds the flux in the corresponding feature at 95 GHz by a factor of four. Gaussian parameters of the spectral features are presented in Table 1.

Figure 2 presents a map of the region described above. It is clear that the masers occupy only the central part of this map. Evidence for emission in the same velocity range as the central emission (centered on 91 km/s with a line width of about 8 km/s) can be seen at the northwest boundary of the map, offset $-540''$ in right ascension and $780''$ in declination. Unfortunately, the maximum of this emission occurs at the edge of the map, and the line flux is only at the $(2-2.5)\sigma$ level. Additional observations with higher signal-to-noise ratio are required to more reliably confirm the detection of this emission and determine the line parameters.

Figure 3 presents a central fragment of the coordinate grid in the vicinity of the maser. The full coordinate grid is presented in Fig. E-4 at the address http://www.asc.rssi.ru/Lit/online1.pdf.[1] Figures E-5 and E-6 present a fragment of the northwest part of the map and the spectrum of the detected feature.

Figure E-7 presents a map of the studied region ($30' \times 30'$) with the masers at the center. The regions of the possible SNR G27.3−0.2 and the SNR G27.4+0.0 (Kes73) are clearly visible at 21 cm. When the map at 21-cm [33] is overlaid on infrared images obtained with the "Spitzer" space telescope (http://www.spitzer.caltech.edu/), we can visually note certain correspondances, for example, between the possible SNR G27.3−0.2 and the maser region (see Figs. E-8 and E-9). The region of G27.4+0.0 (Kes73) either does not emit in the IR or the data are smeared [16].

The emission region of G27.3−0.2 at 8 μm roughly coincides with the corresponding part of the

[1] The letter "E" preceding the figure number indicates that the figure is presented only in electronic form at the indicated site.

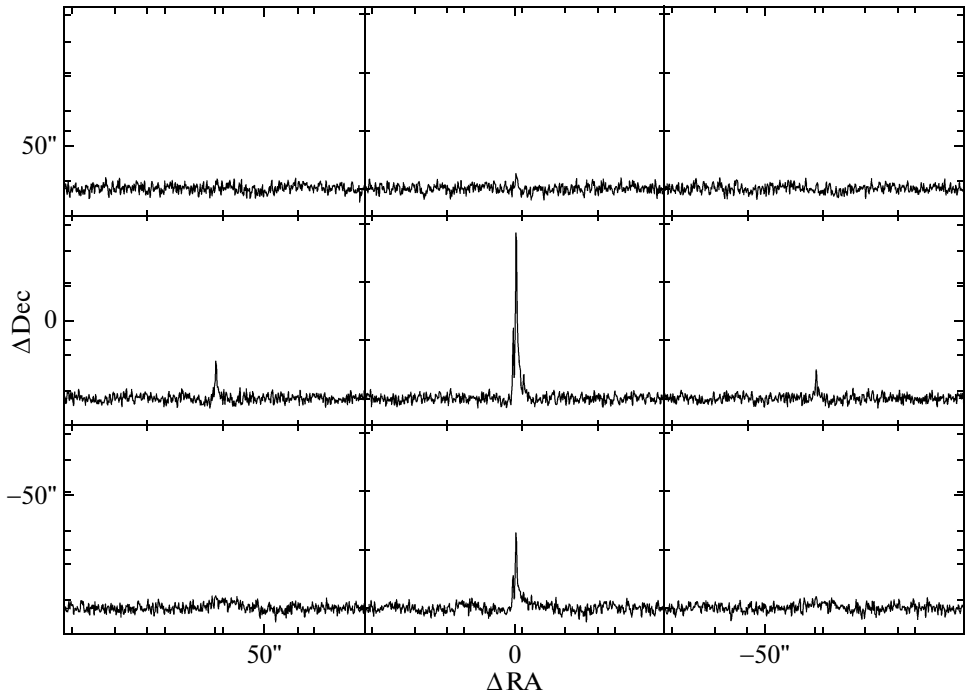

Fig. 3. Coordinate grid for the observations in the $7_0 - 6_1A^+$ methanol-maser ine at 44 GHz in the vicinity of the MMI emission of G27.369−0.164, obtained in steps of 1′ (enhanced fragment of the center).

21-cm map (Figs. E-8 and E-9), forming a ring. This suggests that we see the result of interactions between the interstellar medium and the SNR or its filaments at short IR wavelengths. In other words, it may be that shocks from this SNR have led to densification of molecular condensations, creating the conditions for pumping of the maser. However, it is possible that the compact HII region with which the methanol maser seems to be associated is projected against the possible SNR by chance, and that these objects are actually at different distances from the Earth.

3.1. The Problem of Distance Determination

Distance estimates represent a vulnerable area in the construction of hypotheses about associations between SNRs and maser condensations. Let us consider this question in more detail.

The most precise tool for determining distances in the Galaxy is trigonometric parallax. The Hipparcos mission [34] (http://www.rssd.esa.int/index.php?project) expanded the sphere within which stellar distances can be determined using trigonometric parallax to 300–500 pc. However, this distance is much smaller than the entire Galaxy, and the main distance-determination method remains the analysis of the Galactic rotation curve. The Galactocentric distance $R_0 = 8.5$ kpc and circular speed of the Sun $\theta = 220$ km/s are the values currently adopted by the International Astronomical Union for the calculation of distances based on the Galactic rotation curve.

However, due to the presence of several spiral arms in the Galaxy, the kinematic distances in the first and second quadrants display ambiguities. Removing these ambiguities requires additional observations and the application of criteria enabling the identification of a source with some particular spiral arm. For example, various lines in both emission and absorption are used to determine distances to regions of formation of massive stars. One of the most precise methods is provided by observations of the H110α radio-recombination line together with supplementary data on formaldehyde absorption. This approach enables the derivation of kinematic distances with accuracies of $\pm(0.5–1.0)$ kpc in most cases [35]. At the same time, we should bear in mind various problems in using HI absorpion and emission spectra—clumping of velocities, ambiguity in choosing between near and far distances relative to a tangent point, inhomogeneity in the HI spatial and temperature distribution, etc. [36].

Caswell and Haynes [26] present two distances to the OH-maser region: 6.0 and 11.7 kpc. According to our estimates, the kinematic distance to the methanol-maser region is 5.35 or 10.1 kpc. These distances were determined from the velocity of the brightest feature, which is 93.5 km/s. Ellingsen [13]

Table 1. Derived Gaussian parameters of the maser lines at 44 GHz in G27.369−0.164

Galactic coordinates	IRAS identification	RA(B1950) RA(J2000)	Dec(B1950) Dec(J2000)	Line component number	$\int S_\nu dV$, Jy km/s	V_{LSR}, km/s	Line width, km/s	S_ν, Jy
27.369−0.164	18367−0504	$18^h39^m11.5^s$	$-05°04'24.5''$	1	8.712(1.062)	88.745(0.000)	0.685(0.137)	11.952
		$18^h41^m50.99^s$	$-05°01'28.3''$	2	15.750(0.774)	91.108(0.000)	0.950(0.000)	15.570
				3	70.632(8.208)	93.560(0.116)	2.038(0.167)	32.562
				4	68.886(6.624)	94.466(0.005)	0.767(0.034)	84.366
				5	27.882(1.350)	95.785(0.008)	0.537(0.022)	48.744

adopted the farther distance of 12.5 kpc, at least for the distance to the IR source IRAS 18391-0504.

The kinematic distance to the SNR G27.4+0.0 (Kes73) is from 7.5 to 9.8 kpc, and the presence of a large number of features in the spectra of the SNR and nearby compact HII regions makes it difficult to refine this distance [15].

The distance to the SNR G27.3−0.02 is not known, and the size of G27.3−0.02 is determined less accurately, since it is smeared at 21 cm and the field contains a large number of HII regions [15]. It is possible that this region itself is a diffuse HII region.

If the maser region and the SNRs are located in the same part of a spiral arm, the angular separations of 10′ from the maser region to the SNR G27.4+0.0 (Kes73) and 4.′7 from the maser region to G27.3−0.02 correspond to linear distances from 4 pc to less than 2 pc for the smaller distances, or more than 10 pc for both SNRs for the larger distances.

It is possible that (for the more nearby distances) these sizes could enable the identification of filaments of the SNRs with the maser region. According to the classical scheme, the distance of the MMIs should be of the order of 1 pc, at least from an HII region.

Table 2 presents some characteristics of Kes73, as well as the two SNRs W51 and W44 (data taken from [37, 38]) that are associated with MMI emission. Compared to these, Kes 73 is younger and more compact: it is roughly a factor of 10 smaller than these two older SNRs. It is possible that the object G27.3−0.02, which is closer in terms of its angular distance, exerts a stronger influence on the maser region; however, additional studies are required to test this possibility.

If we could detect appreciable evidence for the influence of an SNR on the formation of the MMI emission, this would enable refinement of the distances to both the star-forming regions and the SNRs.

4. 44-GHz METHANOL EMISSION TOWARD SNRs ASSOCIATED WITH OH(1720) MASER EMISSION

Table 3 presents a full list of MMIs in the northern and southern hemispheres whose coordinates are associated with SNRs. We searched for cases where the two sets of coordinates in the SIMBAD database (http://simbad.u-strasbg.fr/simbad/) agreed to within 10′. The data for the MMIs was taken from the catalogs [9] (a newer version [10] is presented at http://www.asc.rssi.ru/mmI, where references to the original works are also given). Table 3 presents the coordinates of the centers of the SNRs at epochs B1950 and J2000 from the catalog of Green [39] (see also http:/www.mrao.cam.ac.uk/surveys/snrs).

We selected nine objects from the list of northern SNRs in [40] with detected 1720 MHz OH maser emission whose declinations made them accessible to observations on the Onsala telescope. Table 4 presents the Galactic coordinates of these SNRs. For

Table 2. Some characteristics of the SNRs Kes73, W51, and W44

Parameter	SNR*		
	Kes73	W51	W44
Distance, kpc	7.8−9.5	6	2.5
Age, yr	~ 500−1000	$\sim 2\times10^5$	$\sim 3\times10^4$
Angular size, arcmin	4	50×38	25×35
Linear size, pc	9−11	88×66	11×13
Pulsar	Anomalous X-ray	Yes	Yes
Type of remnant	Envelope		Mixed

* See references in text.

Table 3. Full list of MMIs in the northern and southern hemispheres associated with SNRs within 10′

Galactic coordinates of the maser	Source name	RA(B1950) RA(J2000)	Dec(B1950) Dec(J2000)	SNR
318.05+0.09		$14^h49^m52.9^s$	−58°56′47.1″	318.2+00.1
		$14^h53^m42.5^s$	−59°09′00.5″	
345.00−0.22		17 01 38.5	−41 24 59.0	MSC 345.1−0.2
		17 05 09.4	−41 29 04.0	
351.16+0.70	NGC 6334B	17 16 35.5	−35 54 44.0	NGC 6334
		17 19 56.8	−35 57 45.4	
351.24+0.67	GGD 25	17 16 54.5	−35 51 58.0	351.3+00.7
	NGC 6334C	17 20 15.7	−35 54 58.1	NGC 6334
351.446+0.662	NGC 6334I(N)	17 17 33.0	−35 42 04.0	351.3+00.7
		17 20 54.0	−35 45 01.3	351.4+00.7
351.64−1.26		17 25 55.0	−36 37 48.0	351.7−01.2
		17 29 17.9	−36 40 09.2	
358.159+2.649	Sgr A-F	17 42 27.4	−29 02 18.0	00.0+00.0
		17 45 38.1	−29 03 27.7	359.9+00.9
359.981−0.074	Sgr A-A	17 42 41.3	−28 58 18.0	00.0+00.0
		17 45 51.9	−28 59 26.7	359.9+00.9
0.667−0.036	Sgr B2	17 44 10.6	−28 22 03.0	00.7+00.0
	Sgr B2M	17 47 20.3	−28 23 05.2	EQ J174702.6−282733
8.827−0.029		18 02 25.6	−21 19 58.2	08.7−00.1
		18 05 25.4	−21 19 41.0	
10.30−0.15		18 05 57.9	−20 06 26.0	10.3−0.1
		18 08 49.5	−20 05 53.5	
10.47+0.03	W31(1)	18 05 39.6	−19 52 10.8	10.59−0.04
		18 08 37.4	−19 51 39.6	
10.6−0.4	W31C	18 07 30.5	−19 56 28.0	10.2−00.3
	W31(2)	18 10 28.4	−19 55 48.7	10.6−00.4
12.797−0.193	W33-Met	18 11 15.7	−17 56 53.0	12.8−00.2
		18 14 11.0	−17 55 57.4	
15.035−0.674	M17(3)	18 17 31.0	−16 12 50.0	15.0−00.6
	NGC 6618	18 20 24.0	−16 11 27.2	
	AFGL 2124			
26.602−0.220		18 37 58.2	−05 46 28.0	26.6−00.1
		18 40 38.5	−05 43 37.0	
27.286+0.151		18 37 55.1	−05 00 04.2	27.3+00.1
		18 40 34.5	−04 57 13.5	
27.369−0.164		18 39 11.5	−05 04 24.5	27.3−00.2
		18 41 51.0	−05 01 28.3	27.4+00.0

Table 3. (Contd.)

Galactic coordinates of the maser	Source name	RA(B1950) RA(J2000)	Dec(B1950) Dec(J2000)	SNR
29.96−0.02	W43S	$18^h43^m27.1^s$	−02°42′36.0″	29.9−00.1
		$18^h46^m03.9^s$	−02°39′21.6″	
30.69−0.06		18 44 58.9	−02 04 27.0	PKS1844-02
		18 47 34.9	−02 01 06.0	30.3+00.4
				30.8−00.2
30.82−0.06	W43-Main(3)	18 45 11.0	−01 57 57.0	30.8−00.2
		18 47 46.9	−01 54 35.2	30.3+00.4
34.3+0.2	W44	18 50 46.2	01 11 12.0	34.3+00.1
		18 53 18.5	01 14 57.6	
37.479+0.105		18 57 37.8	03 55 38.4	37.6−00.1
		19 00 07.0	03 59 53.0	
43.304−0.208	Mol 97	19 08 52.4	09 02 25.4	43.3−00.2
		19 11 15.9	09 07 27.0	
45.47+0.07		19 12 04.5	11 04 22.5	45.5+00.1
		19 14 25.7	11 09 37.3	
49.472−0.371	W51-Met5	19 21 20.5	14 24 12.0	49.2−00.5
		19 23 38.1	14 30 04.9	
49.473−0.396	W51-Met1	19 21 26.2	14 23 32.0	49.2−00.5
		19 23 43.8	14 29 25.3	
49.48−0.398	W51-Met3	19 21 27.5	14 23 52.0	49.2−00.5
		19 23 45.1	14 29 45.4	
49.481−0.404	W51-Met2	19 21 28.8	14 23 47.0	49.2−00.5
		19 23 46.4	14 29 40.5	
49.485−0.359	W51N	19 21 19.6	14 25 14.95	49.2−00.5
		19 23 37.2	14 31 07.8	
49.49−0.387	W51 e1/e2	19 21 26.2	14 24 43.0	49.2−00.5
	W51 Main/S	19 23 43.8	14 30 36.3	

four of these, evidence for 44-GHz methanol maser emission was obtained earlier; see the last column in Table 4. For the remaining objects, we observed at the coordinates of the SNRs from Table 4, at the velocities of the maxima in the 1720 MHz OH ines. No new methanol maser sources were detected at the 3σ level, which corresponds, on average, to about 2–3 Jy.

We comment individually on the SNRs from Table 4 below. The methanol-maser data were taken from the catalogs [9, 10].

8.7-0.1. This is a known SNR with which the maser 8.67-0.36 can be identified; the velocities of the OH(1720) and MMI emission roughly coincide.

9.7-0.0. A powerful MMII and weak MMI have coordinates close to the SNR, but the velocities of these masers (4–9 km/s) and the velocity of the OH(1720) maser differ strongly; i.e., the SNR is not related to the observed methanol emission.

34.7-0.4, W44. The radial velocities of the OH(1720) maser emission and the nearby methanol maser emission differ by roughly 10 km/s.

Table 4. List of SNRs from [40] within which 1720 MHz OH maser emission has been observed

Galactic coordintes of the SNR	SNR name	RA(B1950) RA(J2000)	Dec(B1950) Dec (J2000)	Map of SNR*	OH(1720) spectrum	V_{LSR} (OH(1720)), km/s**	44 GHz methanol maser***
8.7−0.1		$18^h03^m19^s$	$-21°24'25''$	Y	N	+36	Y
		$18^h06^m19^s$	$-21°24'04''$				
9.7−0.0		18 04 55	−20 33 13	Y	N	+43:	N
		18 07 54	−20 32 45				
16.7+0.1		17 58 05	−14 20 28	Y	Y	+19.9	N, this survey
		18 00 56	−14 20 30				
21.8−0.6	Kes69	17 58 10	−10 05 13	Y	Y	+69.8	N, this survey
		18 00 56	−10 05 15				
31.9+0.0	3C191	18 46 50	−00 59 59	Y	Y	+107	N, this survey
		18 49 25	−00 56 30				
32.8−0.1	Kes78	18 48 51	−00 11 37	Y	Y	+86.1	N, this survey
		18 51 25	−00 08				
34.7−0.4	W44	18 53 30	+01 16 00	Y	Y	+45	Y
		18 56 02	+01 19 57				
49.2−0.7		19 21 00	+14 05 00	N	Y	+70	Y
		19 23 18	+14 10 52				
189.1+3.0	IC 443	06 13 55	+22 30 15	Y	Y	−6	N, this survey
		06 16 56	+22 29 08				
33.7−0.0	(Kes79)****	18 50 15.1	+00 37 00			−	Not at $V_{LSR} = 90$ km/s, this survey
		18 52 48.05	+00 40 43				

* See [14, 23, 40].
** See [40].
*** See references in [9, 10].
**** Unable to find information about OH(1720) maser observations.

49.2-0.7. The new MMI G49.267-0.337 at nearby coordinates was recently discovered toward the Extreme Green Object G49.267-0.337 in [41] at a velocity close to the velocity of the OH(1720) maser.

Let us summarize the new results of our survey.

16.7+0.1, 21.8-0.6 (Kes69), 31.9+0.0(3C191), 32.8-0.1 (Kes78), 189.1+3.0(IC 443). We did not detect any MMI emission toward these SNRs at the coordinates and velocities corresponding to their OH(1720) masers.

33.69-0.01 (Kes79). This SNR is absent from the tables of the latest version of the catalog of Green [39], and we were unable to find data on OH(1720) observations. Since the coordinates of this SNR are very close to the coordinates of Kes78 (according to the SIMBAD database; Table 4), we carried out our 44 GHz observations at a velocity of 90 km/s, which is roughly the velocity of the nearby SNR Kes8. No methanol emission was detected.

These results are presented in column (8) of Table 4.

Thus, based on the observations, we tentatively conclude that the presence of OH(1720) emission is not a sufficient condition for the detection of MMI emission at the coordinates and velocity of the OH maser. It is possible that the most probable candidates for the detection of this type of molecular maser emission will be "missing SNRs;" see, for example, [42]. These should radiate at 2 μm with roughly the same pattern for moving elements of the medium as

that observed by Voronkov et al. [43] in IRAS 16547-4247; i.e., when the flows of matter are not strong enough to support H_2 emission or to prevent the shocks from disrupting complex organic molecules, but are strong enough to pump MMIs.

5. DISCUSSION

The main problem is demonstrating a connection between molecular maser emission in the interstellar medium and an SNR. The most important requirement for this is that the SNR be in the region of the maser condensation; i.e, for each specific region, it is necessary to carry out a spatial continuum study at various wavelengths—in the infrared, radio, optical and X-ray. Emission in radio molecular lines that trace dense gas, motions of material, and shocks must also be studied. Moreover, it is important to distinguish features of the observed methanol-maser line profiles that might testify to the influence of shock fronts. Such features are present in the OH profiles: the presence of maser emission at 1720 MHz, together with the absence of level inversions for other transitions at 1665, 1667, and 1612 MHz. Such so-called Class IIa OH masers have long been known and have been well studied. Studies of SNRs associated with masers of this type began with the pioneering work of Pastchenko and Slysh (see, e.g., [44]). A survey of more modern works is given, for example, in [40].

The absence of MMI emission at the location of OH(1720) emission in six SNRs studied here may indicate that the amount of methanol in the corresponding gas–dust clumps is insufficient for this maser emission. Nevertheless, there is hope that such masers will eventually be detected, since the physical conditions in fragments of the interstellar medium in which OH(1720) maser emission forms and in condensations giving rise to MMI emission are fairly similar: the cooling shock-heated gas has a narrow range of temperatures (25–125 K), high densities to 10^5 cm^{-3}, and column densities of OH molecules 10^{17} cm^{-2} [40]. Methanol condensations have densities of 10^5 cm^{-3}, typical temperatures of 25–100 K, and column densities of methanol of 10^{16}–10^{17} cm^{-2} [45].

Even if there are few MMIs excited by shocks from SNRs, efforts put into studies of these sources will be justified, since they can help impose fairly strict constraints on pumping models, as well as the physical conditions in the maser condensations and the ambient interstellar medium, which can help lead to a better understanding of the physics of masers, the physics of shocks, and the nature of SNRs.

6. CONCLUSION

We have detected 44-GHz Class I methanol-maser emission in the 7_0–6_1A^+ line in the region of active maser emission G27.4–0.2. We have constructed a $27' \times 27'$ 44-GHz map of the vicinity of the maser emission, which shows that the 44-GHz emission forms only within the previously known maser region.

We were not able to draw firm conclusions about the extent to which the two SNRs G27.4+0.0 (Kes73) and G27.3–0.02 influence the formation of the dense region in which the maser emission is generated. As a minimum, this will require large-scale mapping in lines tracing dense gas (CS, NH_3), high-velocity motions of matter (CO), and shocks ($H_2$1-0S(1) at 2.12 μm).

We note especially the lack of detection of OH(1720) emission in the maser region G27.4–0.2—only the usual OH(1665) maser emission was detected, probably providing information about the SNR itself, although, as has been noted in many studies (see references above), the absence of OH(1720) maser emission by itself does not rule out interactions between the SNR and surrounding molecular clouds.

We have searched for 44-GHz MMI emission in six SNRs at the coordinates and velocities of their OH(1720) maser emission. No 44-GHz MMI emission was detected at the 3σ level; i.e., the presence of OH(1720) emission is not a sufficient condition for the detection of this methanol maser emission. More detailed mapping of SNRs in methanol lines is required for a fuller understanding of the meaning of this result.

ACKNOWLEDGMENTS

This work was partially supported by the Russian Foundation for Basic Research (project 10-02-00147-a), the Basic Research Program of the Division of Physical Sciences of the Russian Academy of Sciences "Active Processes and Stochastic Structures in the Universe 2009, 2010," and by the Ministry of Education and Science of the Russian Federation, Federal Targeted Program "Scientific and Science-Education Staff of Innovative Russia (2009–2013)" (state contracts nos. 16.740.11.0155 and 02.740.11.0251). We thank S.V. Kalenskii for help in composing the proposal for telescope time, and the staff of the Onsala Space Observatory (Sweden) for the possibility of observing on the OSO telescope and for help with the observations, in particular P. Bergman and R. Hammargren.

REFERENCES

1. J. M. De Buizer, Mon. Not. R. Astron. Soc. **341**, 277 (2003).
2. M. D. Smith, J. Eisloffel, and C. J. Davies, Mon. Not. R. Astron. Soc. **297**, 687 (1998).
3. R. M. Lees, Astrophys. J. **184**, 763 (1973).
4. D. M. Cragg, K. P. Johns, P. D. Godfrey, et al., Mon. Not. R. Astron. Soc. **259**, 203 (1992).
5. R. Bachiller, S. Liechti, C. M. Walmsley, et al., Astron. Astrophys. **295**, L51 (1995).
6. S. Leichti and C. M. Walmsley, Astron. Astrophys. **321**, 625 (1997).
7. J. L. Caswell, Mon. Not. R. Astron. Soc. **308**, 683 (1999).
8. J. L. Caswell, Mon. Not. R. Astron. Soc. **349**, 99 (2004).
9. I. E. Val'tts and G. M. Larionov, Astron. Rep. **51**, 519 (2007).
10. I. E. Val'tts, G. M. Larionov, and O. S. Bayandina, arXiv:1005.3715v3 [astro-ph.GA] (2010).
11. Bon-Chul Koo and Ji-hyun Kang, Mon. Not. R. Astron. Soc. **349**, 983 (2004).
12. S. V. Polushkin and I. E. Val'tts, Astron. Rep. **54**, 496 (2010).
13. S. P. Ellingsen, Mon. Not. R. Astron. Soc. **359**, 1498 (2005).
14. B. Koralesky, D. A. Frail, W. M. Goss, et al., Astrophys. J. **116**, 1323 (1998).
15. W. W. Tian and D. A. Leahy, Astrophys. J. **677**, 292 (2008).
16. P. W. Gorham, S. R. Kulkarni, and T. A. Prince, Astron. J. **105**, 314 (1993).
17. F. J. Lockman, Astrophys. J. Suppl. Ser. **71**, 469 (1989).
18. P. Lockett, E. Gauther, and M. Elitzur, Astrophys. J. **511**, 235 (1999).
19. Y. Pihlstrom, V. L. Fish, L. O. Sjouwerman, et al., Astrophys. J. **676**, 371 (2008).
20. D. A. Frail, W. M. Goss, E. M. Reynoso, et al., Astron. J. **111**, 1651 (1996).
21. A. J. Green, D. A. Frail, W. M. Goss, and R. Otrupcek, Astron. J. **114**, 2058 (1997).
22. C. L. Brogan, W. M. Goss, J. S. Lazendic, and A. J. Green, Astron. J. **128**, 700 (2004).
23. J. W. Hewitt and F. Yusef-Zadeh, Astrophys. J. **694**, L16 (2009).
24. D. A. Frail, W. M. Goss, and V. I. Slysh, Astrophys. J. **424**, L111 (1994).
25. B. L. Ulich and R. W. Haas, Astrophys. J. Suppl. Ser. **30**, 247 (1976).
26. J. L. Caswell and R. F. Haynes, Austral. J. Phys. **36**, 417 (1983).
27. M. A. Braz and N. Epchtein, Astron. Astrophys. Suppl. Ser. **54**, 181 (1983).
28. L. A. Hanslow, Honours Thesis (Univ. Tasmania, Australia, Tasmania, 1997).
29. S. Zoonematkermani, D. J. Helfand, R. H. Becker, et al., Astrophys. J. Suppl. Ser. **74**, 181 (1990).
30. R. H. Becker, Astrophys. J. Suppl. Ser. **91**, 347 (1994).
31. C. J. Cyganowski, B. A. Whitney, E. Holden, et al., Astron. J. **136**, 2391 (2008).
32. T. Liu, Y.-F. Wu, and K. Wang, Res. Astron. Astrophys. **10**, 67 (2010).
33. J. J. Condon, W. D. Cotton, E. W. Greisen, et al., Astron. J. **115**, 1693 (1998).
34. M. A. C. Perryman, L. Lindegren, J. Kovalevsky, et al., Astron. Astrophys. **323**, L49 (1997).
35. M. Sewilo, C. Watson, E. Araya, et al., Astron. J. **154**, 553 (2004).
36. K. Y. Sanbonmatsu and D. J. Helfand, Astron. J. **104**, 2189 (1992).
37. B.-C. Koo, J.-J. Lee, F. D. Seward, and D.-S. Moon, Astron. J. **633**, 946 (2005).
38. D. P. Cox, R. L. Shelton, W. Maciejewski, et al., Astron. J. **524**, 179 (1999).
39. D. A. Green, Bull. Astron. Soc. India **37**, 45 (2009).
40. J. W. Hewitt and F. Yusef-Zadeh, Astrophys. J. **683**, 189 (2008).
41. C. J. Cyganowski, C. L. Brogan, T. R. Hunter, and E. Churchwell, Astrophys. J. **702**, 1615 (2009).
42. B.-C. Koo, J.-H. Kang, and C. J. Salter, Astrophys. J. **643**, L49 (2006).
43. M. A. Voronkov, K. J. Brooks, A. M. Sobolev, et al., Mon. Not. R. Astron. Soc. **373**, 411 (2006).
44. M. I. Pastchenko and V. I. Slysh, Astron. Astrophys. **35**, 153 (1974).
45. A. M. Sobolev, A. B. Ostrovskii, M. S. Kirsanova, O. V. Shelemei, O. V. Voronkov, and A. V. Malyshev, in *Massive Star Birth: A Crossroads of Astrophysics*, Ed. by R. Cesaroni, M. Felli, E. Churchwell, and M. Walmsley (Cambridge Univ., 2005), p. 174; arXiv:astro-ph/0601260 (2006).

Translated by D. Gabuzda